

## Lensing of Stars by Spherical Gas Clouds

B.T. Draine

*Princeton University Observatory, Peyton Hall, Princeton, NJ 08544; draine@astro.princeton.edu*

### ABSTRACT

If the Galaxy contains  $\sim 10^{11} M_{\odot}$  in cold gas clouds of  $\sim$ Jovian mass and  $\sim$ AU size, these clouds will act as converging lenses for optical light, magnifying background stars at a detectable rate. The resulting light curves can resemble those due to gravitational lensing by a point mass, raising the possibility that some of the events attributed to gravitational microlensing might in fact be due to “gaseous lensing”. During a lensing event, the lens would impose narrow infrared and far-red  $H_2$  absorption lines on the stellar spectrum. Existing programs to observe gravitational microlensing, supplemented by spectroscopy, can therefore be used to either detect such events or place limits on the number of such gas clouds present in the Galaxy.

*Subject headings:* dark matter – galaxies: halos – galaxies: ISM – galaxies: the Galaxy – gravitational lenses – ISM: clouds

## 1. Introduction

A number of authors have proposed that the Galaxy could contain a hitherto-unrecognized population of small, cold, dense self-gravitating gas clouds, in numbers sufficient to contribute an appreciable fraction of the gravitational mass of the Galaxy (Pfenniger, Combes, & Martinet 1994; Gerhard & Silk 1996; Combes & Pfenniger 1997).

Walker & Wardle (1998; hereafter WW98) pointed out that if such clouds existed in the Galactic halo, each would have an ionized envelope which could explain the “Extreme Scattering Events”, or “ESEs”, (Fiedler et al. 1987) during which extragalactic point radio sources occasionally undergo substantial frequency-dependent amplification and deamplification, apparently due to refraction by a plasma “lens” moving across the line-of-sight. WW98 proposed that the observed frequency of such ESEs could be explained if there was a population of  $\sim 10^{14}$  cold self-gravitating gas clouds, with mass  $M \approx 10^{-3} M_{\odot}$ , and radius  $R \approx 3$  AU.

Gerhardt & Silk (1996) and WW98 noted that if the clouds were opaque, their presence would have been revealed by existing stellar monitoring programs studying gravitational “microlensing” (Paczynski 1986; see the review by Paczynski 1996, and references therein), as these experiments would have detected occultation events of duration  $\sim R/200 \text{ km s}^{-1} \approx 40$  days. Such occultation events have not been reported. However, the hypothesized clouds could be essentially transparent at optical wavelengths: they could have formed from primordial gas, or, if formed from gas containing metals, the grains could have sedimented to form a small core.

In this *Letter* we point out that even transparent clouds would have lensing effects which would be detectable by the stellar monitoring studies currently underway to study gravitational lensing by compact objects in our Galaxy. Existing data can thus test the hypothesis that cold gas

clouds contribute an appreciable fraction of the mass of the Galaxy.

## 2. Density Profile

We consider nonrotating polytropic models for self-gravitating H<sub>2</sub>-He gas clouds of radius  $R$ . The polytropic index  $n$  ( $T \propto \rho^{1/n}$ ) is assumed to be in the range  $1.5 < n < 5$ ; for  $n < 1.5$  the cloud would be convectively unstable, while for  $n \geq 5$  the central density is infinite. We do not expect  $T(r)$  and  $\rho(r)$  to be accurately described by a polytropic model, but a slight rise in temperature toward the interior may be reasonable since the interior will be heated by high energy cosmic rays, with the few cooling lines [e.g., H<sub>2</sub>0-0S(0) 28.28  $\mu\text{m}$ , or HD 0-0R(1) 112  $\mu\text{m}$ ] very optically thick. Furthermore, these polytropes have  $T(R) = 0$ , so the density structure near the surface is unphysical. Table 1 gives various properties for H<sub>2</sub>-He polytropes, including the half-mass radius  $r_h$ ,  $T_c \equiv T(0)$ ,  $T_h \equiv T(r_h)$ , and  $\rho_c \equiv \rho(0)$  and  $\rho_h \equiv \rho(r_h)$  relative to the mean density  $\langle \rho \rangle \equiv 3M/4\pi R^3$ .

## 3. Gaseous Lensing

For  $\rho \lesssim 10^{-2} \text{ g cm}^{-3}$ , the refractive index  $m$  is

$$m(\lambda) = 1 + \alpha(\lambda)\rho \quad ; \quad (1)$$

$\alpha(4400 \text{ \AA}) = 1.243 \text{ cm}^3 \text{ g}^{-1}$  and  $\alpha(6700 \text{ \AA}) = 1.214 \text{ cm}^3 \text{ g}^{-1}$  for H<sub>2</sub>/He gas with 24% He by mass (AIP Handbook 1972).

For small deflections, a light ray with impact parameter  $b$  will be deflected through an angle

$$\phi(b) = -2\alpha b \int_b^{\infty} \frac{dr}{(r^2 - b^2)^{1/2}} \frac{d\rho}{dr} \quad . \quad (2)$$

There is a small additional gravitational deflection (Henriksen & Widrow 1995), but this is negligible compared to gaseous refraction.

Let  $D_{\text{SL}}$  and  $D_{\text{LO}}$  be the distance from source to lens, and from lens to observer. If  $b_0$  is the distance of the lens center from the straight

line from source to observer (see Fig. 1), then the apparent distance  $b$  of the image from the lens is given by the lensing equation

$$b - b_0 = D\phi(b) \quad , \quad D \equiv \frac{D_{\text{SL}}D_{\text{LO}}}{D_{\text{SL}} + D_{\text{LO}}} \quad . \quad (3)$$

For a point source, the image magnification is given by

$$M(b) = \frac{|b|}{b_0} \frac{1}{1 - D\phi'(b)} \quad , \quad (4)$$

$$\phi'(b) \equiv \frac{d\phi(b)}{db} = -2\alpha \int_0^\infty dz \left[ \frac{b^2}{r^2} \frac{d^2\rho}{dr^2} + \frac{z^2}{r^3} \frac{d\rho}{dr} \right] \quad . \quad (5)$$

where  $r^2 = b^2 + z^2$ . For a given  $b_0$  there will be an odd number  $N(b_0)$  of solutions  $b_i(b_0)$ ,  $i = 1, \dots, N$ . The total amplification  $A(b_0) = \sum_{i=1}^N M(b_i)$ . The “trajectory” of the lens relative to the source is characterized by a “source impact parameter”  $p$  and a displacement  $x$  along the trajectory; for any  $x$  we have  $b_0 = (p^2 + x^2)^{1/2}$ , and the “light curve” is just  $A(b_0)$  vs.  $x$ .

We define a “strength” parameter

$$S \equiv \frac{\alpha\langle\rho\rangle D}{R} = 3.55 \left( \frac{M}{10^{-3}M_\odot} \right) \left( \frac{\text{AU}}{R} \right)^4 \left( \frac{D}{10 \text{ kpc}} \right) \quad . \quad (6)$$

When  $S$  is of order unity, large amplifications (and deamplifications) are possible even for  $b_0/R$  of order unity, whereas if  $S \ll 1$ , appreciable amplification only occurs for  $b_0 \ll R$ .

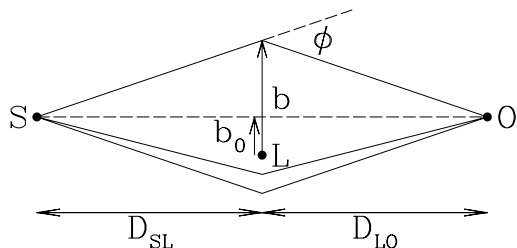


Fig. 1.— Geometry of lensing. S is the source, the center of the lens is at L, and O is the observer.

#### 4. Sample Light Curves

For each polytropic index we define the critical strength  $S_c(n)$  to be the value of  $S$  such that for  $b_0 = 0$  there are 3 images for  $S > S_c$  and one image for  $S < S_c$ . Values of  $S_c$  are given in Table 1.

For each case with  $S > S_c$  we define the critical source impact parameter  $b_{0c}(S)$  such that there is one image for  $b_0 > b_{0c}$ , and 3 images for  $b_0 < b_{0c}$ . For  $S > S_c$  a light curve for which  $p < b_{0c}$  will have “cusps” at the points where  $b_0 = b_{0c}$ , as two images either appear (for  $|x|$  decreasing) or merge and disappear (for  $|x|$  increasing).

Figures 2–4 show light curves for lenses with polytropic indices  $n = 2, 3$ , and 4, respectively. The following general behavior is found: (1) For  $S \lesssim 0.3S_c$  the lensing is weak, with peak amplification  $A(0) \lesssim 2$ ; (2) For  $0.7S_c \lesssim S < S_c$  the peak amplification can be very large, even though only one image is formed; (3) For  $S_c < S \lesssim 5S_c$  the peak amplification is very large, and light curves with  $p < b_{0c}$  have conspicuous cusps where the amplification for a point source is infinite; (4) For  $S \gtrsim 10S_c$ , the cusps become weak because image merging only occurs for  $b_0 \approx R$ , and the two merging images are faint.

In each figure we also show, for comparison, an ideal “gravitational lensing” light curve fitted<sup>1</sup> to the light curve for  $p = 0.01R$ . Note that for  $S < S_c$  (no cusps present) or  $S \gtrsim 10S_c$  ( $b_{0c} \gtrsim 0.7R$ , so that the cusps are weak) there is considerable similarity between the gravitational lensing and gaseous lensing light curves.

#### 5. Discussion

For purposes of discussion, we adopt the  $n = 3$  polytropic model (with  $\rho_c = 54\langle\rho\rangle$ ) as a guide. For  $S \gtrsim 0.5S_c$  we obtain amplifications  $A(p) >$

<sup>1</sup> The gravitational lensing light curve is fitted by requiring it to have the same peak amplification  $A_{max}$  and to have the same width at  $A = A_{max}^{1/2}$ .

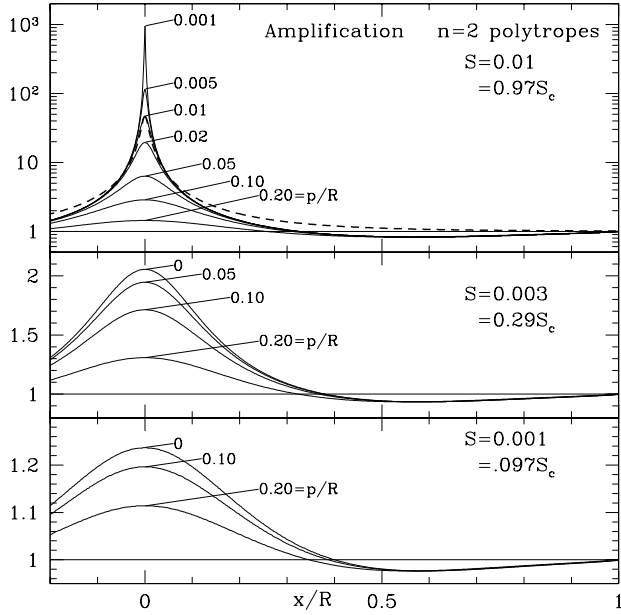


Fig. 2.— Light curves for transparent polytropes of index  $n = 2$  and lensing strength  $S = 0.001$ ,  $0.003$ , and  $0.01$ . Also shown is an ideal “gravitational lensing” light curve (broken line) fitted to the light curve for  $p = 0.01R$ . For these three cases, with  $S < S_c$ , the gaseous lens light curves resemble gravitational lensing light curves when the amplification is large, but show systematic differences at low amplification; in particular, every gaseous lens has a range of  $b_0$  where it deamplifies.

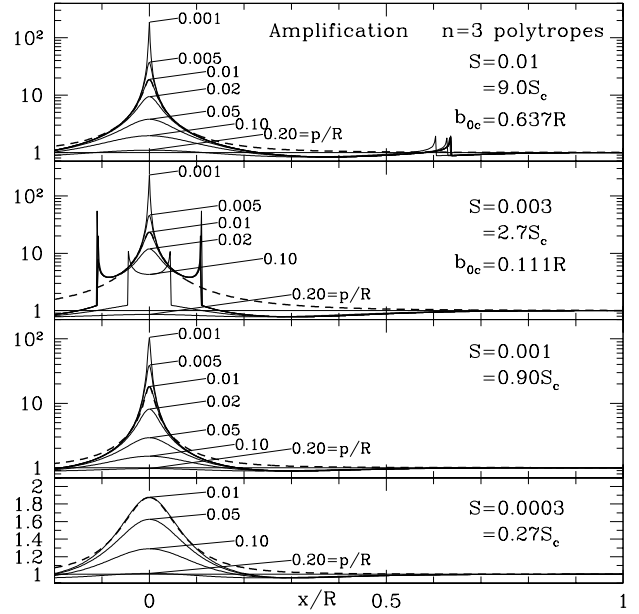


Fig. 3.— Same as Fig. 2 but for  $n = 3$ . When  $S > S_c$ , light curves with  $p < b_{0c}(S)$  contain conspicuous cusps (see text).

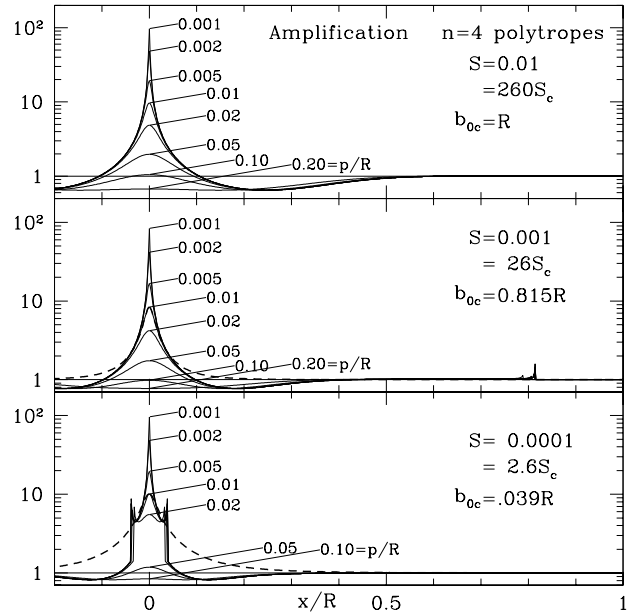


Fig. 4.— Same as Fig. 2 but for  $n = 4$ .

1.5 for  $p \lesssim 0.1R$  (see Fig. 3).

### 5.1. Lensing Event Rate

Fiedler et al. (1994) report 9 ESEs in 594 source-years of monitoring. Two events (0954+658 and 1749+096, with durations  $\sim 0.35$  yr) have radio light curves suggestive of lensing by the ionized atmosphere of a spherical cloud, implying a rate  $\dot{P}_{\text{ESE}} \approx 2/594 \approx 3 \times 10^{-3} \text{ yr}^{-1}$  per source, and a “covering factor”  $f_{\text{ESE}} \approx \dot{P}_{\text{ESE}} \times 0.35 \text{ yr} \approx 1 \times 10^{-3}$ . If the plasma envelope extends to  $\sim 1.5R$ , then from the 0.35yr duration of the radio events we estimate  $R \approx 200 \text{ km s}^{-1} \times 0.35 \text{ yr} / 2 \approx 7 \text{ AU}$ .

The neutral cloud covering factor would then be  $f \approx f_{\text{ESE}} / (1.5)^2 \approx 5 \times 10^{-4}$ , and the rate per source of optical lensing events with  $p < 0.1R$  is

$$\dot{P}_{\text{OL}} \approx (0.1R/1.5R)\dot{P}_{\text{ESE}} \approx 2 \times 10^{-4} \text{ yr}^{-1} \quad . \quad (7)$$

The optical light curve would have a characteristic time scale  $\sim 0.2R / (200 \text{ km s}^{-1}) \approx 10$  days, short compared to the observed lensing events toward the LMC (Alcock et al. 1997), but within the detectable range: with an effective exposure of  $\sim 2 \times 10^6$  source-years the absence of  $\sim 10$  day events exceeding the  $A > 1.75$  MACHO threshold implies an upper limit of  $\sim 1.5 \times 10^{-6} \text{ yr}^{-1}$ , 100 times smaller than  $\dot{P}_{\text{OL}}$  from eq. (7)! We can therefore exclude the possibility that the typical cloud can produce amplifications  $A \gtrsim 2$ : the gas clouds associated with ESEs must have  $S \lesssim 0.3S_c$  for  $D \approx 10 \text{ kpc}$ . Thus

$$M \lesssim 8.5 \times 10^{-5} M_{\odot} (R/\text{AU})^4 (10 \text{ kpc}/D) S_c \quad . \quad (8)$$

### 5.2. Other Limitations

If the clouds are at a typical distance of 10 kpc and contribute a covering fraction  $f \approx 5 \times 10^{-4}$  (see above), the total mass in clouds should not exceed  $\sim 10^{11} M_{\odot}$ :

$$M \lesssim 1 \times 10^{-5} M_{\odot} (R/\text{AU})^2 \quad . \quad (9)$$

A third requirement is that the gravitational binding energy of gas particles near the surface

exceed the thermal kinetic energy per particle for plausible surface temperature  $T \approx 10 \text{ K}$ :

$$M \gtrsim 6 \times 10^{-5} M_{\odot} (R/\text{AU}) \quad . \quad (10)$$

These 3 conditions are plotted in Fig. 5. We see that the parameters favored by WW98 –  $M = 10^{-3} M_{\odot}$ ,  $R = 3 \text{ AU}$  – are ruled out by both eqs. (8) and (9). However, an allowed region does remain, including  $M \approx 10^{-3} M_{\odot}$ ,  $R \approx 10 \text{ AU}$ .

### 5.3. Demagnification

For  $p > b_{0c}$  (*i.e.*, no cusps), light curves for spherical gaseous lenses bear considerable similarity to light curves for gravitational lensing. As a consequence, it would not be trivial to distinguish gravitational lensing from gaseous lensing purely on the basis of optical light curves, particularly since departures from ideal gravitational lensing of point sources by point masses are anticipated due to blending with other stars, lensing by stars with planetary or stellar companions, and sources of finite angular extent. The most conspicuous difference in the light curves is the fact that gaseous lensing always has a range of  $b_0$  values for which  $A < 1$ , unlike gravitational lensing. Accurate photometry could either detect such deamplification, or place a limit on it. Note that for lenses with  $S \ll 1$  the deamplification is very slight: for example, for  $n = 3$  and  $S < S_c$ ,  $A > 0.88$ . Thus accurate photometry would be required to either detect such deamplification or obtain a useful limit.

### 5.4. Spectroscopy

The cold molecular gas will be nearly transparent at infrared and optical frequencies, but could be detected through  $\text{H}_2$  absorption lines. The characteristic  $\text{H}_2$  column density is

$$N(\text{H}_2) \approx \frac{M/R^2}{2.64 m_{\text{H}}} \approx 2 \times 10^{25} \left( \frac{M}{10^{-3} M_{\odot}} \right) \left( \frac{10 \text{ AU}}{R} \right)^2 \text{ cm}^{-2} \quad . \quad (11)$$

The  $\text{H}_2$  will be mainly in the  $(v, J) = (0, 0)$  and  $(0, 1)$  levels. Quadrupole vibrational absorption

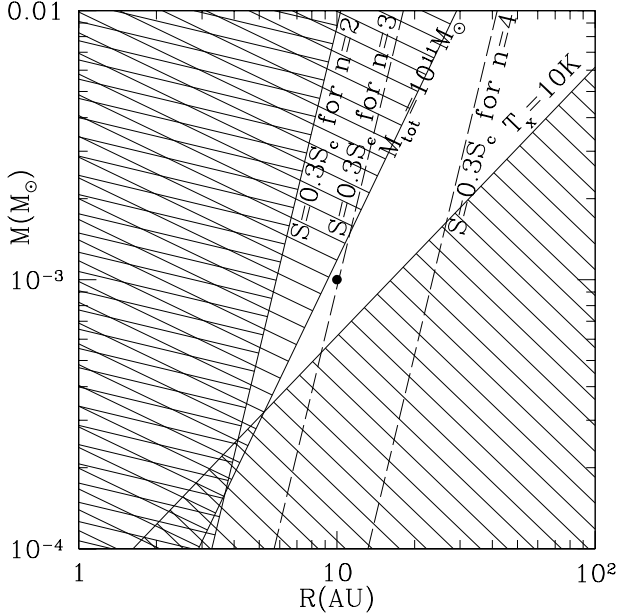


Fig. 5.— Allowed values of  $M$  and  $R$ , for gas clouds at  $D \approx 10$  kpc. Below the line “ $T_x = 10$  K” the surface layers of the polytrope would be unbound for  $T = 10$  K. Above the line “ $S = 0.3S_c$ ” the cloud would be capable of amplification  $A \gtrsim 2$  and hence this region is ruled out by searches for optical lensing toward the LMC. Above the line  $M_{tot} = 10^{11} M_\odot$  clouds with a covering fraction  $f = 5 \times 10^{-4}$  would contribute more than  $10^{11} M_\odot$ .

lines out of these two levels are listed in Table 2, with line-center absorption cross sections  $\sigma_0$  computed neglecting pressure broadening and assuming only thermal broadening at  $T = 20$  K. For the estimated column densities in eq. (11) we see that the 1-0 transitions would have central optical depths  $\tau \approx 10^3$ . While the overtone transitions are weaker, the increased stellar brightness near  $\sim 8300 \text{ \AA}$  plus sensitive CCD detectors may make the 3-0 transitions best to use. Detection of these absorption features would both confirm the gaseous nature of the lens and determine its radial velocity, expected to be  $\sim 200 \text{ km s}^{-1}$  if the lens belongs to the halo as proposed by WW98.

### 5.5. Chromaticity

The optical dispersion results in a slightly larger value of  $S$  in the blue. However, noting the similarity in light curves for  $S = 0.01$  and  $S = 0.001$  for  $n = 3$ , it is clear that changing  $S$  by 0.8% will be expected to produce only a very slight increase in amplification (“blueing”). If, however, caustics are present in the light curve, the caustics will occur at different times for different colors, which would be detectable with multicolor photometry with good time resolution.

The increased amplification at shorter wavelengths is counteracted by Rayleigh scattering, which will redden light passing through the cloud (WW98). The Rayleigh scattering cross section is  $\sim 8.4 \times 10^{-29} (\mu\text{m}/\lambda)^4 \text{ cm}^2$ , resulting in reddening of a magnified star by  $E(B - V) \approx 1.3 \times 10^{-27} N(\text{H}_2) \text{ cm}^2$ , giving  $E(B - V) \approx 0.03$  for  $N(\text{H}_2)$  from eq. (11).

If the lensed star happened to be bright in the ultraviolet, the gaseous lens would completely block the ultraviolet radiation shortward of  $\sim 1200 \text{ \AA}$  through the damping wings of the Lyman and Werner band transition of  $\text{H}_2$ , which overlap to form an opaque continuum shortward of  $\sim 1110 \text{ \AA}$  for  $N(\text{H}_2) \gtrsim 10^{21} \text{ cm}^{-2}$  (Draine & Bertoldi 1996). Since most target stars are far too faint to be detected in the vacuum ultraviolet, however, it seems unlikely that this absorp-

tion could be observed.

## 6. CONCLUSIONS

It is not obvious how cold self-gravitating gas clouds with the properties suggested by WW98 might have formed, or whether such clouds would be stable for  $\sim 10^{10}$  yr. However, if they do exist, WW98 show that they could solve two long-standing problems: (1) their ionized envelopes could account for some of the “Extreme Scattering Events”; and (2) they could contain the “missing” baryons in the Galaxy. It is notable that these same clouds could ameliorate a third problem: the fact that microlensing searches detect a larger number of amplification events toward the LMC than expected for lensing by stars and stellar remnants. Some of these events could be due to gaseous lensing. Indeed, lensing by the hypothesized clouds would be so frequent that existing programs to observe gravitational microlensing can already place strong limits on the cloud parameters (see Fig. 5), but clouds with  $M \approx 10^{-3}M_{\odot}$  and  $R \approx 10$  AU are still allowed.

With a predicted lensing rate  $\dot{P}_{\text{OL}} \approx 2 \times 10^{-4} \text{ yr}^{-1}$ , the typical lens must be weak, with  $S \lesssim 0.3S_c$ . The distribution of cloud properties and distances could produce occasional strong gaseous lensing events with  $S \gtrsim 1$ , perhaps accounting for some of the events attributed to gravitational microlensing.

For non-caustic lensing, the dispersive effects of the gas would produce slightly larger amplification in the blue, but this is counteracted by Rayleigh scattering by the  $\text{H}_2$ . A number of quadrupole lines of  $\text{H}_2$  would be detectable in absorption during the lensing event; this would be the most unambiguous signature of “gaseous lensing”.

Existing programs to observe gravitational lensing, supplemented by spectroscopy during lensing events, can therefore be used to either detect gaseous lensing events or place limits on the number of  $\sim 10^{-3}M_{\odot}$   $\text{H}_2$  clouds in the Galaxy.

I am grateful to Bohdan Paczynski for helpful comments, and to Robert Lupton for the availability of the SM package. This work was supported in part by NSF grant AST-9619429.

## REFERENCES

- Alcock, C., et al. 1997, *ApJ*, 486, 697
- American Institute of Physics Handbook 1972, ed. D.E. Gray, Table 6e-5
- Combes, F., & Pfenniger, D. 1997, *A&A*, 327, 453
- Draine, B.T., & Bertoldi, F. 1996, *ApJ*, 468, 269
- Fiedler, R., Dennison, B., Johnston, K.J., & Hewish, A. 1987, *Nature*, 326, 675
- Fiedler, R., Dennison, B., Johnston, K.J., Waltman, E.B., & Simon, R.S. 1994, *ApJ*, 430, 581
- Gerhard, O., & Silk, J. 1996, *ApJ*, 472, 34
- Henriksen, R.N., & Widrow, L.M. 1995, *ApJ*, 441, 70
- Paczynski, B. 1986, *ApJ*, 304, 1
- Paczynski, B. 1996, *ARAA*, 34, 419
- Pfenniger, D. Combes, F., & Martinet, L. 1994, *A&A*, 285, 79
- Walker, M., & Wardle, M. 1998, *ApJL*, 498, L125 (WW98)

---

This 2-column preprint was prepared with the AAS L<sup>A</sup>T<sub>E</sub>X macros v4.0.

TABLE 1  
POLYTROPIC MODELS

$n$	$\rho_c/\langle\rho\rangle$	$\rho_h/\langle\rho\rangle$	$r_h/R$	$T_c^a$	$T_h^a$	$S_c$
1.5	5.9907	2.3228	0.52118	13.19	7.52	.026
2	11.403	3.5602	0.43921	14.74	7.81	.0103
2.5	23.407	5.9809	0.36004	17.14	8.38	.0037
3	54.183	11.416	0.28331	20.93	9.29	.00111
3.5	152.88	26.539	0.20879	27.45	10.76	.00028
4	622.41	88.183	0.13650	40.80	13.32	$3.9 \times 10^{-5}$
4.5	6189.5	703.43	0.06671	81.60	19.31	$2 \times 10^{-6}$

<sup>a</sup>For  $M = 10^{-3}M_\odot$  and  $R = 10$  AU.

TABLE 2  
H<sub>2</sub> ABSORPTION LINES

line	$\lambda(\mu\text{m})$	$\sigma_0(\text{cm}^2)$	line	$\lambda(\mu\text{m})$	$\sigma_0(\text{cm}^2)$
1-0 Q(1)	2.4066	$3.3 \times 10^{-24}$	3-0 Q(1)	0.8500	$8.8 \times 10^{-27}$
1-0 S(0)	2.2233	$7.7 \times 10^{-24}$	3-0 S(0)	0.8275	$3.4 \times 10^{-26}$
1-0 S(1)	2.1218	$4.3 \times 10^{-24}$	3-0 S(1)	0.8153	$2.5 \times 10^{-26}$
2-0 Q(1)	1.2383	$2.0 \times 10^{-25}$	4-0 Q(1)	0.6567	$5.6 \times 10^{-28}$
2-0 S(0)	1.1896	$5.9 \times 10^{-25}$	4-0 S(0)	0.6437	$2.8 \times 10^{-27}$
2-0 S(1)	1.1622	$3.9 \times 10^{-25}$	4-0 S(1)	0.6370	$2.4 \times 10^{-27}$